AN EVALUATION OF THE APERIODIC AND FLUCTUATING INSTABILITIES FOR THE PASSIVE RESIDUAL HEAT REMOVAL SYSTEM OF AN INTEGRAL REACTOR

HAN-OK KANG*, YONGHO LEE and JUHYEON YOON
Korea Atomic Energy Research Institute
150 Deokjin-dong, Yuseong-gu, Daejeon, 305-353, Korea
*Corresponding author. E-mail : hanokang@kaeri.re.kr

Received August 4, 2005
Accepted for Publication December 1, 2005

Convenient analytical tools for evaluation of the aperiodic and the fluctuating instabilities of the passive residual heat removal system (PRHRS) of an integral reactor are developed and results are discussed from the viewpoint of the system design. First, a static model for the aperiodic instability using the system hydraulic loss relation and the downcomer feedwater heating equations is developed. The calculated hydraulic relation between the pressure drop and the feedwater flow rate shows that several static states can exist with various numbers of water-mode feedwater module pipes. It is shown that the most probable state can exist by basic physical reasoning, that there is no flow rate through the steam-mode feedwater module pipes. Second, a dynamic model for the fluctuating instability due to steam generation retardation in the steam generator and the dynamic interaction of two compressible volumes, that is, the steam volume of the main steam pipe lines and the gas volume of the compensating tank, is formulated and the D-decomposition method is applied after linearization of the governing equations. The results show that the PRHRS becomes stabilized with a smaller volume compensating tank, a larger volume steam space and higher hydraulic resistance of the path a_{ct}. Increasing the operating steam pressure has a stabilizing effect. The analytical model and the results obtained from this study will be utilized for PRHRS performance improvement.

KEYWORDS : Flow Instability, Passive Residual Heat Removal System, Once-through Steam Generator, D-decomposition Method, Integral Teactor

1. INTRODUCTION

SMART-P is an advanced modular integral type pressurized water reactor whose major RCS components, such as the main coolant pump, helical-coiled steam generator, and pressurizer, are contained in a reactor vessel [1,2]. A Passive Residual Heat Removal System (PRHRS) is installed to prevent overheating and over-pressurization of the primary system for non-LOCA events. The PRHRS removes the core decay heat and sensible heat by natural circulation of a two-phase fluid in the case of emergency events such as unavailability of the feedwater supply or loss of off-site power. The PRHRS consists of four independent trains with 50 % capacity each. Two trains are sufficient to remove the decay heat generated from the reactor core. Each train includes a Heat eXchanger (HX) submerged in a Refueling Water Tank (RWT), fail-open inlet/outlet isolation valves and a Compensating Tank (CT).

Fig. 1 shows a schematic flow diagram for one train of the SMART-P PRHRS. If a PRHRS actuation signal is generated from the plant protection system, the PRHRS inlet/outlet valves are opened and the isolation valves for the main steam and feedwater lines are closed. An intermediate circuit consisting of steam generators (SG), a steam line, HX and feedwater line is formed. The steam generated from the SG is sent to the HX and condensed there. The density difference between the steam and feedwater lines supplies the necessary driving force for the feedwater. The CT supplies enough feedwater into the flow path during the initial operational period and compensates variation of the system pressure and feedwater volume. The current PRHRS design features ensure a makeup of the SG with the feedwater stored in the CT at the necessary intensity during the initial stage of an accident scenario, owing to the compressed gas energy.The PRHRS gets stabilized into the assigned operation mode with minimum dynamic fluctuation of the steam pressure [3]. The two-phase condition is ensured for most of the operating time, thus guaranteeing efficient heat removal from the primary circuit, with sufficient enough reserve at the SG heat-exchange surface. The RWT serves as the final heat sink of the PRHRS operation. Table 1 shows the main design parameters of the SG

Table 1. Main Design Parameters of the SG and PRHRS of SMART- Corresponding to One Train

Parameter	Value
Steam Generator*	
Primary operating pressure (MPa)	14.7
Primary inlet/outlet temperature (°C)	310/274
Primary coolant flow rate (kg/sec)	90
Secondary operating pressure (MPa)	3.45
Secondary inlet/outlet temperature (°C)	50/282
Feedwater flow rate (kg/sec)	6
Pressure drop for SG cassette (MPa)	1.17
SG active height (m)	1.11
Heat transfer area of SG (m^2)	21.6
PRHRS**	
Operating pressure (MPa)	3.5
Operating flow rate (kg/sec)	0.5
HX active height (m)	1.2
CT total volume (m^3)	0.8
Elevation of HX active part over SG active part (m)	3.55
RWT coolant temperature (°C)	100
Heat transfer area of HX (m^2)	7.5

* The described values are for the rated condition.

** The described values are for PRHRS operating condition.

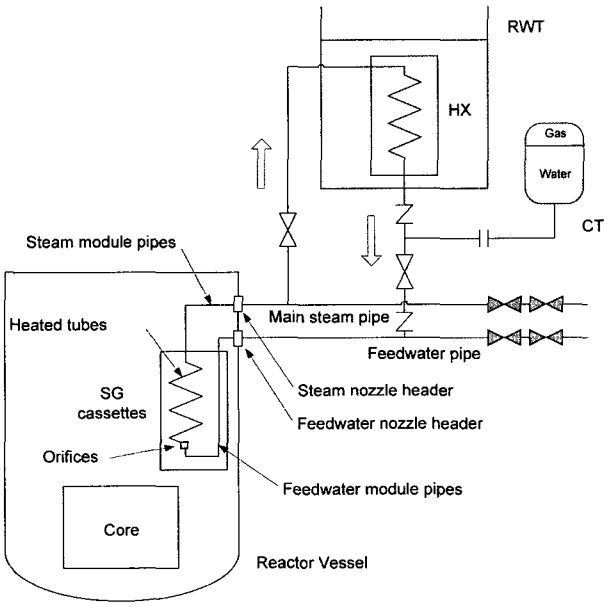

Fig. 1. Schematic Flow Diagram of SMART-P PRHRS

and the PRHRS of SMART-P corresponding to one train.

Owing to the efficiency of the PRHRS, several studies have been conducted with the aim of utilizing it in the residual heat removal system of nuclear plants [4-8]. Russian integral reactors, such as ATEC-200 and KLT-40, which have been developed for local district heating and desalination, depend on a passive secondary cooling system to remove the residual heat in the event of total loss of power [4,5]. Boiling water reactors such as SWR1000 and SBWR utilize a passive core cooling concept with horizontal or vertical heat exchangers [6,7]. Numerous experimental studies to evaluate the various aspects of passive heat removal systems have been conducted [9-12]. Kim and Lee carried out an experimental study on the flow instabilities within a semi-closed two-phase natural circulation loop [9]. They found that the circulation becomes stable when the frictional resistance at the expansion-tank line becomes larger, especially at high heat-flux and high inlet sub-cooling conditions [9]. Other studies related to condensing heat transfer and the non-condensable gas effect have been reported [10-12].

Three SG cassettes per train are installed inside the reactor vessel and each of them is composed of steam/feedwater nozzle headers, module pipes, and heated tubes. The SG cassette is connected with the main steam and feedwater pipe lines through the nozzle located at the reactor vessel, as shown the Fig. 1.

In the SMART-P, the steam and feedwater nozzles are located above the SG cassettes. This arrangement is partially for the elimination of lower penetration of the vessel and partially for easier routing of the feedwater pipes. However, this design feature inevitably requires a slightly longer feedwater module pipe submerged in the primary coolant, thereby bringing about feedwater preheating in front of the tube orifices. For the rated condition, temperature increase of the feedwater through the feedwater module pipe is confined within the design limit, while the value will be significant enough for the low flow condition, especially for the PRHRS operating mode. Aperiodic instability caused by the presence of the downcomer feedwater pipes may affect the system performance and shorten the component design lifetime.

Another feature of the PRHRS is the availability of two compressive volumes in the intermediate circuit: the steam volume of the main steam pipe lines and the gas volume of the compensating tank. In addition, the PRHRS causes SG operation under low flow rate conditions beyond the design limits of the operating range (10 ~ 100 %) with a relatively high hydraulic resistance of the steam lines. Fluctuating instability originates from the dynamic interaction of the two compressible volumes and a retardation mechanism of steam generation in the SG. Fig. 2 shows the experimental data for the compensating tank level and the flow rate of the intermediate circuit from a Russian reference, where two variables oscillate with the same period [13]. This kind of oscillation reduces the efficiency

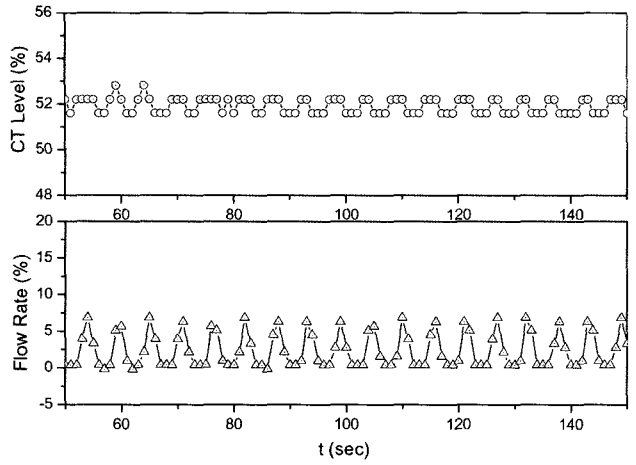

Fig. 2. Experimental Data for the Compensating Tank Level and Circuit Flow Rate

of the heat removal and introduces a high thermal load onto the structure material, and thus its occurrence should be prevented in advance in the design stage. Aperiodic and fluctuating instability mechanisms may occur in the heat-exchange tubes and circuits due to working fluid boiling, which necessitates taking into account their impact on the PRHRS operability and effectiveness in an analytical validation.

The objectives of the present study are to develop convenient analytical tools for the aperiodic and fluctuating instabilities, and to evaluate the effect of each PRHRS design parameter on the system stability. First, a static model for the aperiodic instability using the system hydraulic loss relation and the downcomer feedwater heating equations is developed and the effect of the SG inlet temperature on the system stability is discussed. Second, a dynamic model for the fluctuating instability owing to steam generation retardation and the dynamic interaction of two compressible volumes is formulated and the D-decomposition method is applied after linearization of the governing equations.

2. APERIODIC INSTABILITY

2.1 A Model for One Representative Feedwater Module Pipe Assumption

The flow rate for the PRHRS operating condition is much lower than the value for the rated condition, which induces boiling at the feedwater module pipes accompanied by aperiodic instability. A condition of aperiodic instability for the two-phase flow circuit is satisfied for the multi-valued hydraulic curve for the general case [14]. In the case of the SMART-P PRHRS, the following hydraulic curve can be multi-valued depending on the flow regime of the downcomer feedwater pipes (and orifice) of the SG:

$$H_{circuit} = F(\xi_{circuit}) \tag{1}$$

where $H_{circuit}$, $\xi_{circuit}$ are the hydrostatic head and the normalized flow rate for the rated value. For a qualitative assessment, eighteen feedwater module pipes of three SGs can be represented by one equivalent feedwater module pipe. The normalized flow rate through the SG feedwater pipes ($\xi_{boundary}$), when the feedwater is heated to the saturation temperature, is determined from the following equation:

$$\xi_{boundary} = \frac{U_{orifice}\{T_{1C} - (T_s + T_{SGinlet})/2\}}{G_{SG}^0(I_s' - I_{SGinlet})} \tag{2}$$

In the above equation, $U_{orifice}$ is a heat transfer factor from the primary circuit (T_{1C}-coolant temperature) to the feedwater and is composed of a heat transfer coefficient and a heat transfer area. T_s and I_s' are the feedwater temperature and enthalpy in the saturation line with the pressure of the intermediate circuit respectively. $T_{SGinlet}$ and $I_{SGinlet}$ are the feedwater temperature and enthalpy at the SG inlet nozzle, respectively. G_{SG}^0 is a nominal feedwater flow rate through the SG. For each assigned steam pressure, it is possible to plot two hydraulic curves using the real parameters of the steam generator cassette. The first curve, with feedwater heating to $I < I_s'$ (100% water-mode downcomer feedwater pipes and orifices in the SG) is determined when $\xi_{circuit} > \xi_{boundary}$. The second curve (with 100% steam-mode downcomer feedwater pipes and orifices in the SG) is determined when $\xi_{circuit} < \xi_{boundary}$.

Qualitative characteristics of the resultant hydraulic curve are shown in Fig. 3. Two curves and the hydrostatic head are shown the figure. The hydraulic curve is multi-valued, that is, two values of the flow rate achieved during operation of the feedwater pipes in the steam and water modes (points A and B) correspond to the assigned values of the hydrostatic head (horizontal line) in the circuit. Fig. 3 shows that during transition of the feedwater pipe from the water mode to the steam mode, the flow rate can be significantly reduced.

2.2 A Realistic Approach with Several Numbers of Feedwater Module Pipes

The hydraulic curve in Fig. 3 was obtained on an assumption of simultaneous changing of the fluid state in all the SG feedwater module pipes and orifices. However,

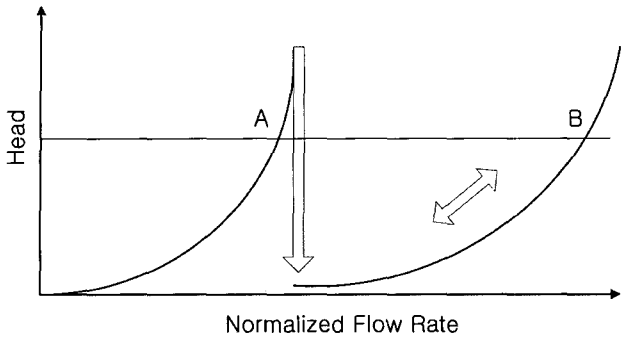

Fig. 3. Hydraulic Curve for Single Feedwater Module Pipe

for the general case, there is a possibility of intermediate operation modes with a part of the steam-mode feedwater modules and orifices. With the assigned circuit flow rate, $\xi_{circuit}$, the steaming of a part of the feedwater pipes and orifices tends to increase the flow rate of the remaining feedwater pipes and orifices, and hence the value of the remaining pipes may exceed the boundary values, $\xi_{boundary}$.

For a quantitative specification of this statement, it is necessary to use an analytical model with Fig. 4, which takes into account branching of the circuit into two downcomer sections in the SG, one (with fraction a) operating in the water mode and the other (with fraction 1-a) operating in the steam mode.

The corresponding mathematical model of the intermediate circuit thermo-hydraulics includes two balance equations between the hydrostatic head and hydraulic losses. One is for the circuit and the other for the equivalent downcomer sections:

$$(L_{HX}+h_{HX})+h_{SG}\times\Gamma(a)=\left\{\Delta P^0_{steam}\left(\frac{\gamma^0_{steam}}{\gamma_{steam}}\right)+\Delta P^0_{water}\right\}\xi^2_{circuit}+\frac{\Delta P_{water}}{a^2}\cdot|\xi_{water}|\cdot\xi_{water} \quad (3)$$

$$h_{SG}\times\Gamma(a)=\frac{\Delta P_{water}}{a^2}\cdot|\xi_{water}|\cdot\xi_{water}-\frac{\Delta P_{steam}}{(1-a)^2}\cdot|\xi_{steam}|\cdot\xi_{steam} \quad (4)$$

Feedwater heating through the water-mode and steam-mode feedwater module pipes of the SG are expressed as follows:

$$I_{water}=I_{SGinlet}+\frac{U_{orifice}\cdot a\cdot\{T_{1C}-(T_{water}+T_{SGinlet})/2\}}{G^0_{SG}\cdot\xi_{water}} \quad (5)$$

$$I_{steam}=I_{SGinlet}+\frac{U_{orifice}\cdot(1-a)\cdot(T_{1C}-T_{steam})}{G^0_{SG}\cdot\xi_{steam}} \quad (6)$$

and continuity:

$$\xi_{circuit}=\xi_{water}+\xi_{steam} \quad (7)$$

where

$\Delta P_{water}=\Delta P^0_{orifice}(\gamma^0_{water}/\gamma_{water})$,
$\Delta P_{steam}=\Delta P^0_{orifice}(\gamma^0_{water}/\gamma_{steam})$,
$\gamma_{water}=\gamma'(I_{water}, P)$, $T_{water}=T(I_{water}, P)$,
$\gamma_{steam}=\gamma''(P)$, $T_{steam}=T_s(P)$,

$\Gamma(a)=\begin{cases}1, \text{if } a>0\\ 0, \text{if } a=0\end{cases}$ - modified step function, $a\in[0,1]$;

In the above equations, ΔP^0 denotes the pressure drop for the rated condition. Pressure drops for the steam and water sections of the overall PRHRS are represented by ΔP^0_{steam} and ΔP^0_{wate}, respectively, and the value for the feedwater module section including the orifice by $\Delta P^0_{orifice}$.

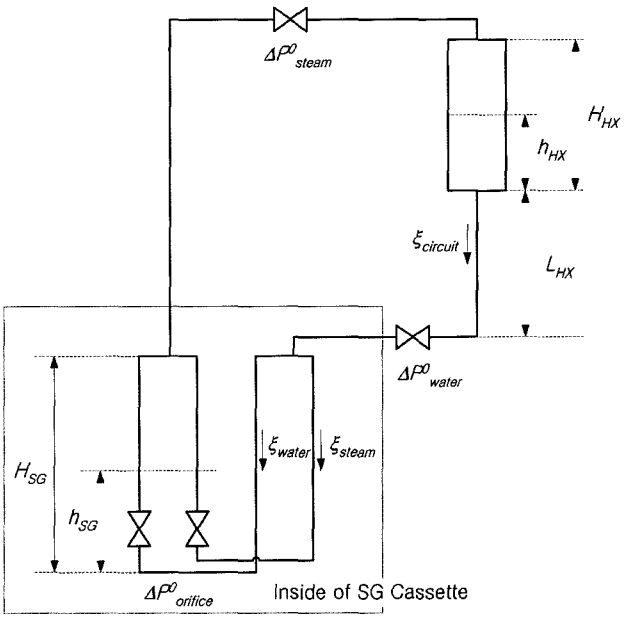

Fig. 4. Schematic Diagram of PRHRS for the Aperiodic Instability Analysis

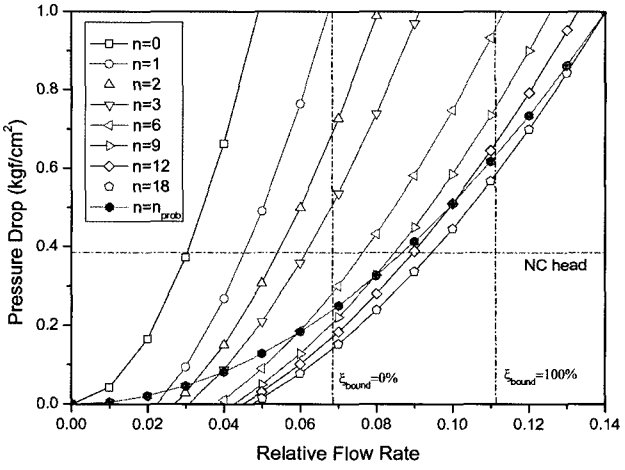

Fig. 5. Hydraulic Curves, $F(\zeta_{bound}, a)$ for the Various a Values

γ, ζ, T, I, H and L denote the density, normalized flow rate, temperature, enthalpy, component height and elevation, respectively. Superscript *0* is the nominal value and subscripts *water* and steam refer to the orifices operating in the water and steam modes. h_{SG} and h_{HX} are the operating water levels for the SG and the HX, respectively.

The left side of Equation 3 corresponds to the hydrostatic head of the intermediate circuit and the right side to any pressure loss of the intermediate circuit except the hydrostatic head. The modified step function $\Gamma(a)$ is introduced to reflect the condition of the feedwater module pipes. The hydrostatic head for the feedwater module pipes is considered only if they are filled with water. Equation 4 is a momentum balance equation for the internal circulation of the SG cassette.

When varying a portion of the orifices operating in the water mode, a (within range [0,1], including $a=0$ and $a=1$), a hydraulic curve of the circulation circuit can be expressed in the following form:

$$(L_{HXC} + h_{HXC}) = F(\xi_{circuit}, a) \tag{8}$$

Fig. 5 presents the analysis results of Equation 8 for P^0_{steam}=3MPa, $T_{SGinlet}$=150°C. The required parameters for this analysis are obtained from the steady state design program, which calculates the PRHRS state variables from the given primary and environmental conditions [15]. The figure also shows $\zeta_{bound}^{0\%}$, the flow rate corresponding to steaming of all the feedwater module pipes and orifices in the SG, and $\zeta_{bound}^{100\%}$, the flow rate corresponding to 100% non-steaming of the feedwater module pipes and orifices in the SG. $\zeta_{bound}^{0\%}$ and $\zeta_{bound}^{100\%}$ are obtained with equations (5) and (6), respectively. The feedwater module pipes is purely in the water mode for $\zeta_{circuit} > \zeta_{bound}^{100\%}$ and in the steam mode for $\zeta_{circuit} < \zeta_{bound}^{0\%}$. Hence, there is no possibility of aperiodic instability for these ranges of $\zeta_{circuit}$. On the contrary, the feedwater module pipes can be filled with steam or water alternately with some aperiodic tendency for $\zeta_{bound}^{0\%} < \zeta_{circuit} < \zeta_{bound}^{100\%}$. In the figure, n is a times N, that is, the number of feedwater module pipes and orifices operating in the water mode (N-total number of feedwater module pipes). From Fig. 5, it can be seen that with the assigned value of the hydrostatic head ($L_{HX} + h_{HX}$) in the area restricted by the curve, $F(\zeta_{circuit}, a=1)$ for the flow rate of $\zeta_{circuit} > \zeta_{circuit}^{100\%}$ and by the curve, $F(\zeta_{circuit}, a=0)$ for the flow rate of $\zeta_{circuit} < \zeta_{bound}^{100\%}$, there can be many possible operational states that differ from each other according to the portion of orifices operating in the water mode, a. The number of orifices operating in the water mode varies between 6 and 18.

The number of orifices operating in the water mode is not evenly distributed in this range but has a preferable value due to physical constraints. Fig. 5 also shows the most probable curve $F(\zeta_{circuit}, a_{probable})$, along which there is no flow rate through the steam-mode feedwater module pipes. If we assume that the flow rates for the steam-mode feedwater module pipes are zero, then Equation 3 is simplified as follows:

$$F(\xi_{ciruit}, a_{probable}) = \left\{ \Delta P^0_{steam} \left(\frac{\gamma^0_{steam}}{\gamma_{steam}} \right) + \Delta P^0_{water} \right\} \xi^2_{circuit} \tag{9}$$

Equation 9 shows that the circuit flow rate does not depend on the SG pressure drop characteristics. If $a < a_{probable}$, then the flow rate through the steam-mode feedwater module pipes is positive. Due to the relatively larger frictional loss of the steam-mode feedwater module, the flow rate through it will be diminished and a approaches $a_{probable}$. On the contrary, if $a > a_{probable}$, then the flow rate through the steam-mode feedwater module pipes is negative. In this situation, steam is mixed with the feedwater in the feedwater nozzle header. This will disturb the operation of the water-mode feedwater module pipes and, as a consequence, a again approaches $a_{probable}$. In a real situation, the value of a is thought to fluctuate around $a_{probable}$. Fig. 5 shows that twelve feedwater modules are operating in the water mode and the other remaining modules in the steam mode. If the temperature of the feedwater increases, the number of feedwater modules operating in the water mode decreases, and every module changes into steam mode under $\zeta_{bound}^{0\%}$. Conversely, reduction of the feedwater temperature induces an increase of the feedwater module number in the water mode, and every module changes into water mode over $\zeta_{bound}^{100\%}$. If the PRHRS operates with some number of steammode feedwater module pipes allowing aperiodic

instability, the feedwater module pipe walls and related structures will undergo large amplitude thermal cycling, and a resultant shorter component lifetime. Hence, it is desirable that all the feedwater modules operate in the water mode without aperiodic instability from the viewpoint of a component's integrity. For this purpose, system designers may consider increasing the HX elevation for a larger hydrostatic head or increasing the HX heat transfer area for lower feedwater temperature. However, complete elimination of the steamed feedwater module is a far too restrictive requirement to achieve with a reasonable geometry and component limitation. Accordingly, system designers generally allow for the occurrence of aperiodic instability for the PRHRS operation mode and place a limitation on the frequency of the PRHRS actuation, which will reduce the usage factor of the PRHRS components.

3. FLUCTUATING INSTABILITY

3.1 Analytical Models for Fluctuating Instability

The PRHRS is a cooling system operating in the two-phase condition. The hydrostatic head for the fluid circulation is supplied from the weight difference of the hydrostatic columns in the riser and downcomer sections. The momentum for the fluid circulation is closely related to two-phase heat transfer, evaporation in the SG and condensation in the HX. Hence, the PRHRS can operate in an instable mode depending on the selection of the design parameters. The availability of two compressible volumes in the intermediate circuit (one steam volume formed by steam regions of the intermediate circuit and the other gas volume in the form of a gas reservoir in the CT) and SG operation under a low flow rate with relatively high hydraulic resistance of the steam line supply adequate conditions for the fluctuating instability.

In the case of unheated single-phase pipe flow, the whole process is purely hydro-dynamic and the system response is governed by the speed of the pressure wave. Hence, the inlet and outlet flow rates do not have any phase difference. On the contrary, in the case of a once-through steam generator, the heat transfer from the primary side and the resultant heating and boiling processes of the feedwater have a strong effect on the hydraulic characteristics of the system, and vice versa. As a result of his interaction between the heat transfer and the hydraulic characteristics, the system response for the inlet perturbation is not instantaneous. If an arbitrary flow rate perturbation is given to the inlet of the SG, there exists some retardation or time delay for the outlet steam flow rate variation. This retardation mechanism can induce flow oscillation for particular conditions such as low feedwater flow rate [16].

It is known that the period of the possible oscillations of the parameters in the intermediate circuit under fluctuating instability conditions has the time order of a working medium passing a heated section [16]. The period in the liquid section is much longer than the period in the two-phase mixture section due to the relatively low density of the mixture as compared to the liquid, and thus the total time of the heated section passing time is determined by the period in the liquid heated section.

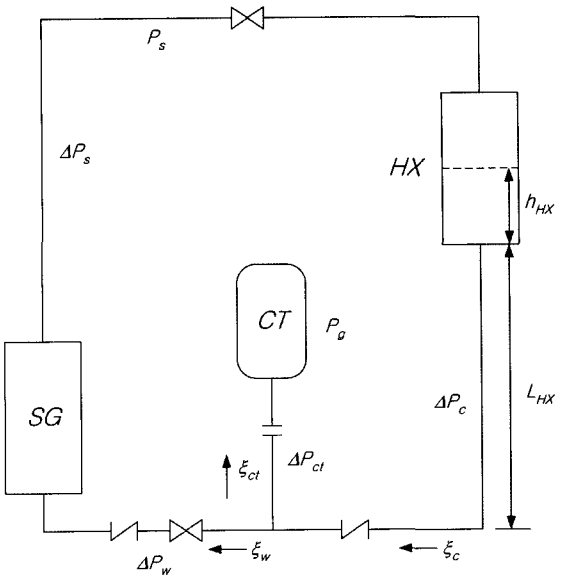

Fig. 6. Schematic Diagram of PRHRS for the Fluctuating Instability Analysis

In this study, the fluctuating instability of the PRHRS will be formularized based on the dynamic interaction of two compressible volumes and a retardation mechanism of steam generation in the SG, and hence the governing equations for the instability analysis will be derived by focusing on these two phenomenal characteristics. An analytical model is developed with Fig. 6, where the variables are defined so as to take into account the existence of two compressible volumes and retardation of steam generation in the SG [17]. The steam flow rate at the SG outlet ξ_s is determined by the water flow rate at its inlet, ξ_w, with a lag for a period of the passing the subcooled region of SG, τ_{ec}.

$$\xi_s(t) = \xi_w(t-\tau_{ec}) \tag{10}$$

The steam pressure P_s is assumed to be only a function of the fluid mass inventory m_f in the intermediate circuit, except the CT with a time lag, τ_{circ}.

$$P_s = P_s[(m_f(t-\tau_{circ})] \tag{11}$$

The fluid mass inventory m_f can be expressed as the following equation:

$$\frac{dm_f(t)}{dt} = -G_w^0 \cdot \xi_{ct} \tag{12}$$

After combining the above two equations and some rearrangement, we can obtain a normalized steam pressure variation equation in the differential form.

$$\tau_s \cdot \frac{dp_s(t)}{dt} = -\xi_{ct}(t - \tau_{circ}) \tag{13}$$

For the gas pressure variation equation, we begin with a state equation of the CT gas volume.

$$p_g \cdot V_g = p_g \cdot (V_{ct} - V_w) \tag{14}$$

The gas mass inventory in the CT is invariant.

$$m_g = V_g \cdot \gamma_g = const \tag{15}$$

First, differentiating Equation 15 and then introducing Equation 14 into the differential equation, we can obtain a normalized gas pressure variation equation in the differential form.

$$\tau_g \cdot \frac{dp_g(t)}{dt} = \xi_{ct}(t) \tag{16}$$

Momentum equations for the CT-SG path and intermediate circuit have the following forms:

$$a_{ct} \cdot \xi_{ct}(t) = p_s(t) - p_g(t) - a_s \cdot \xi_w^2(t - \tau_{ec}) - a_c \cdot \xi_c^2(t) + H_{nc0} \tag{17}$$

$$a_w \cdot \xi_w^2(t) + a_s \cdot \xi_w^2(t - \tau_{ec}) + a_c \cdot \xi_c^2(t) = H_{nc0} \tag{18}$$

And the continuity equation (balance of the flow rates from the point of a CT connection to the circuit) is as follows:

$$\xi_{ct}(t) = \xi_c(t) - \xi_w(t) \tag{19}$$

In the above equations, the following designations are used.

- $p_j(t)$: normalized pressures ($p_j = p_j / p_j^0$), s–steam, g–gas
- ξ_j : normalized flow rates ($\xi_j = G_j / G_w^0$), w–water, s–steam, c–condensate, ct–compensating tank
- H_{nc0} : normalized hydrostatic head, $(L_{hx}+h_{hx}) / p_s^0$
- a_j : normalized hydraulic losses $\Delta p_j / p_n^0$, where Δp_j is hydraulic losses at corresponding sections
- τ_j : time constants of the steam and gas compressible volumes

$$\tau_s = P_s^0 / (G_w^0 \, dP_s/dm_f), \quad \tau_g = (V_g \cdot P_s^0 \, d\rho_g/dP_g \cdot \gamma_w/\rho_g)/G_w^0$$

Superscript 0 refers to the value for the rated condition. Derivative dP_s/dm_f is determined on the basis of a static dependency and derivative $d\rho_g/dP_g$ – based on the equation of an ideal gas condition. The required parameters for this analysis are obtained from the steady state design program, which calculates PRHRS state variables from the given primary and environmental conditions [15]. The parameter τ_{ec} denotes the time for the working fluid's passage through the subcooled region of the SG. Its value is obtained by dividing the water mass in the subcooled region by the flow rate through the intermediate circuit. Since an introduction of several lags complicates the analysis, it is further assumed that τ_{circ} is equal to τ_{ec}; that is, all the lags in the heat exchangers are neglected.

3.2 Application of D-Decomposition Method

The D-decomposition method is used to attain better understanding during the analysis of the system stability, where the coefficients space of the obtained characteristic equation is divided into stable and unstable areas [18]. After linearization of equations (10), (13), (16), (17) and (18), and their Laplace conversion, the following characteristic equation is obtained:

$$s \cdot [a_{ct} C + 2\xi_0 a_c a_w] + C \cdot (\tau_s^{-1} e^{-s\tau_{ec}} + \tau_g^{-1}) = 0 \tag{20}$$

where $C = a_w + a_s e^{-s\tau_{ec}} + a_c$

In the above equation, ξ_0 denotes the static flow rate level for ξ_w. At $a_{ct} \rightarrow \infty$, i.e. at the CT isolation from the circuit, Equation 16 is reduced to the following equation:

$$(a_w + a_s \cdot e^{-s\tau_{ec}} + a_c) \cdot s = 0 \quad (21)$$

If we substitute $s = j \cdot \omega$, where ω is a circular frequency and j is $\sqrt{-1}$, then we can obtain two equations for the real and imaginary parts of Equation 21 with one singular equation (s=0).

$$\text{Re}: \; a_w + a_c + a_s \cdot \cos(\omega \cdot \tau_{ec}) = 0 \quad (22a)$$

$$\text{Im}: \; a_s \cdot \omega \cdot \sin(\omega \cdot \tau_{ec}) = 0 \quad (22b)$$

Equation 22a requires that $\omega \cdot \tau_{ec}$ be equal to 0, π, 2π, ... If we assume that the resonance period is twice that of τ_{ec}, then the conditions of the overall-circuit circulation stability (by the steam generation retardation mechanism) can be expressed in the following form:

$$a_w + a_c > a_s \quad (23)$$

with a resonance frequency at the stability boundary $\omega = \pi/\tau_{ec}$. This criterion requires that for stable operation, the hydraulic resistance of the circuit on the water side should be higher than the resistance on the steam side, if there is no CT in the system.

In a general case, the resistance is $a_{ct} < \infty$. Substituting $s = j \cdot \omega$ from Equation 20 after separation of the actual and imaginary parts, two parametric equations are obtained for the two parameters τ_s^{-1} and τ_g^{-1}, characterizing the rigidity of the compressible volumes.

$$\tau_s^{-1} = \frac{x[B(a_{ct}B + 2\xi_0 a_c a_w) + a_s a_{ct} a_c \sin^2 x]}{\tau_{ec} \sin x (B^2 + a_s^2 \sin^2 x)}$$

$$\tau_g^{-1} = \frac{-x[2\xi_0 a_c a_w (B\cos x - a_s \sin^2 x) + a_{ct} a_c a_s \cos x \sin^2 x]}{\tau_{ec} \sin x (B^2 + a_s^2 \sin^2 x)}$$

$$- \frac{x[a_{ct} B^2 \cos x + a_{ct} B \sin^2 x (a_c - a_s)]}{\tau_{ec} \sin x (B^2 + a_s^2 \sin^2 x)}$$

$$\text{where } x = \omega \cdot \tau_{ec}, \; B = a_w + a_s \cos x + a_c \quad (24)$$

and also an equation of the singular line (at s = 0):

$$\tau_s^{-1} + \tau_g^{-1} = 0 \quad (25)$$

Fig. 7 presents the analysis results of the stability boundary in the plane of the parameters τ_s^{-1} and τ_g^{-1} for fixed steam pressure. The stability areas are located to the left of the boundary curves, where the resonance period varies between $2 \cdot \tau_{ec}$ and $4 \cdot \tau_{ec}$. Fig. 7 also indicates the positions of the working points with various gas volumes in the CT. During the analysis of the working point positions in

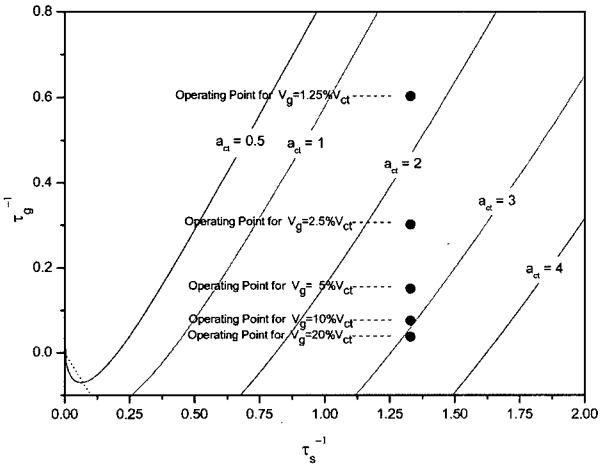

Fig. 7. Stability Boundary in Plane of Parameters τ^{-1}_s and τ^{-1}_g for the Fixed Operating Pressure

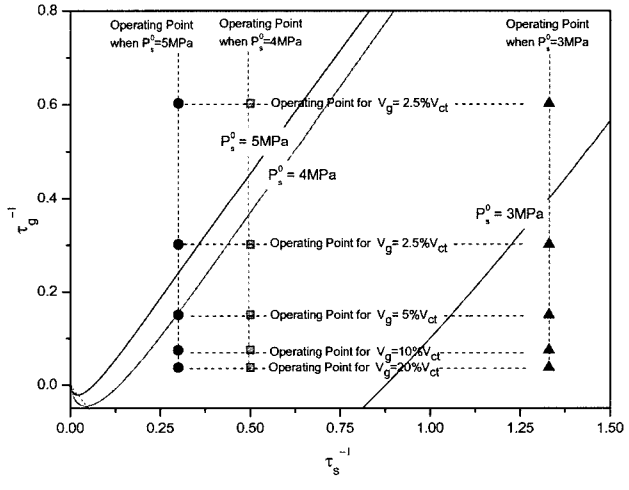

Fig. 8. Stability Boundary in Plane of Parameters τ^{-1}_s and τ^{-1}_g for the Fixed a_{ct}/a_s Ratio

the parameter plane τ_s^{-1} and τ_g^{-1}, the gas volume in the CT varied from 1.25 $\%V_{ct}$ to 20 $\%V_{ct}$. The analysis of the obtained results shows that the instability caused by the dynamic interaction of two compressible volumes in the intermediate circuit is promoted by the following:

- Increase of τ_s^{-1} (decrease of steam volume)
- Reduction of τ_g^{-1} (achieved when the gas volume in the CT increases)
- Reduction of the hydraulic resistance of path a_{ct}

The last item corresponds to the experimental results of Kim and Lee [9]. The stability boundaries for the fixed a_{ct}/a_s ratio (a_{ct}/a_s=1) and the positions of the working points with various CT gas volumes for 3, 4, 5 MPa steam pressures are shown in Fig. 8. The figure indicates that the operating points are located further to the left and at higher positions relative to the stability boundary, which means the stability is increased as the steam pressures increase.

3. CONCLUSIONS

In this paper, simple and convenient analytical tools for the evaluation of the aperiodic and fluctuating instabilities of the PRHRS were developed. First, a static model for the aperiodic instability using the system hydraulic loss relation and the downcomer feedwater heating equations was developed. The hydraulic relation between the pressure drop and feedwater flow rate showed that several static states are possible with varying number of water-mode feedwater module pipes. The analysis also indicated that the system can operate around the curve $F(\zeta_{circuit}, a_{probable})$, along which there is no flow rate through the steam-mode module pipes. In a real situation, the value a is thought to fluctuate around $a_{probable}$. The downcomer energy conservation equations supply two limit flow rates, $\zeta_{bound}^{0\%}$ and $\zeta_{bound}^{100\%}$, over which only steam or water exist in the feedwater module pipe. If the PRHRS operates with a flow rate lower than $\zeta_{bound}^{100\%}$, the SG internal components will undergo large amplitude thermal cycling, which will induce shorter SG cassette lifetime. It is very difficult to completely eliminate the occurrence of aperiodic instability with a practical system configuration, and hence system designers generally allow for the occurrence of aperiodic instability for the PRHRS operation mode and place a limitation on the frequency of the PRHRS actuation.

Second, a dynamic model for fluctuating instability owing to steam generation retardation and dynamic interaction of two compressible volumes, that is, the steam volume of the main steam pipe lines and the gas volume of the compensating tank, was formulated and the D-decomposition method was applied as a stability analysis tool after linearization of the governing equations. The results showed that the PRHRS becomes stabilized for a smaller compensating tank volume, a larger steam space volume, and a higher hydraulic resistance of path act. The increase of the operating steam pressure also had a stabilizing effect. The analytical model and results obtained from this study will be utilized for the detailed design of the SMART-P PRHRS.

REFERENCES

[1] M.H. Chang, J. W. Yeo, S. Q. Zee, D. J. Lee, K. B. Park, I. S. Koo, H. C. Kim, J. I. Kim, Basic design report of SMART, KAERI/TR-2142/2002, KAERI, Daejeon, Korea, 2002.

[2] S.H. Kim, K.K. Kim, J.W. Yeo, M.H. Chung and S.Q. Zee, Design verification program of SMART, Proceedings of the GENES4/ANP2003 Kyoto, Japan, September 15–19, 2003.

[3] Y.J. Chung, S. H. Yang, H.C. Kim and S. Q. Zee, "Thermal hydraulic calculation in a passive residual heat removal system of the SMART-P plant for forced and natural convection conditions," Nucl. Eng. Des., Vol. 232, No. 3, pp. 277-288, 2004.

[4] O.B. Samoilov, V.S. Kuul, V.A. Malamud and G.I. Tarasov, "Integral nuclear power reactor with natural coolant circulation Investigation of passive RHR system," Nucl. Eng. Des. Vol., 165, pp. 259–264, 1996.

[5] F.M. Mitenkov and V.I. Polunichev, "Small nuclear heat and power co-generation station and water desalination complexes on the basis of marine reactor plants," Nucl. Eng. Des., Vol., 173, pp. 183-191, 1997.

[6] A. Schaffrath, E.F. Hicken, H. Jaegers, H.-M. Prasser, "Operation conditions of the emergency condenser of the SWR1000," Nucl. Eng. Des., Vol. 188, pp. 303-318, 1999.

[7] B.S. Shiralkar, M. Alamgir, J.G.M. Andersen, "Thermal hydraulic aspects of the SBWR design," Nucl. Eng. Des., Vol. 144, No. 2, pp. 213-222, 1993.

[8] S.J. Cho, B.S. Kim, M.G. Kang and H.G. Kim, "The development of passive design features for the Korean Next Generation Reactor," Nucl. Eng. Des.,Vol. 201, pp. 259-271, 2000.

[9] J.M. Kim and S.Y. Lee, "Experimental observation of flow instability in a semi-closed two-phase natural circulation loop," Nucl. Eng. Des., Vol. 196, pp. 359-367, 2000.

[10] H. Uchida., A. Oyama and Y. Togo, "Evaluation of post-incident cooling systems of light-water power reactors," Proc. Int. Conf. on the Peaceful Uses of Atomic Energy, 3rd conf., Geneva, Switzerland, Vol. 13, pp. 93-103, 1964.

[11] S.J. Kim, "Turbulent film condensation of high pressure steam in a vertical tube of Passive Safety Condensation System," Korea Advanced Institute of Science and Technology, Ph. D. thesis, 2000.

[12] K.M. Vierow and V.E. Schrock, "Condensation in a natural circulation loop with non-condensable gases - Part 1- heat transfer," Proc. Int. Conf. on Multiphase Flows '91, Tsukuba, Japan, 1991.

[13] O.B. Klochkov, M.A. Bolshukhin, V.S. Danilovsky, A.V. Kulikov and A.V. Davydov, Final report for analysis of PRHRS for SMART-P reactor, OKBM, 2004.

[14] F.J. Moody, The Thermal-Hydraulics of a Boiling Water Nuclear Reactors, ANS, 1977.

[15] H.O. Kang, Performance Analysis Report for PRHRS H/EX, DOOSAN, 2005.

[16] H. Nariai, M. Kobayashi, T. Matsuoka, Y. Ito, I. Aya, "Flow instabilities in a once-through steam generator," Boiler dynamics and control in nuclear power station, BNES, London, 1979.
[17] I.I. Morozov and V.A.Gerliga, "Stability of boiling devices," Atomizdat, Moscow, 1969.
[18] D.D. Siljak, Nonlinear System-The parameter Analysis and Design, John Wiley & Sons, Inc. 1969.